

ment of C IV, Ly α and N V and from limits on He II derived from the FORS and ISAAC spectra we were able to set constraints on the metallicity in SDSS 1030+0524 and SDSS 1306+0356. The metallicity turns out to be much higher than the solar value. Comparison with models for the formation of metals (e.g. Hamann & Ferland 1999) indicates that stars must have been forming for several hundred million years to produce all the metals observed. Therefore the first stars must have formed around the active nucleus at redshift ~ 8.5 or higher. Note also that the inferred age of the stars is much longer than the age of the quasar derived in the previous section, even considering the uncertainty of both estimates.

The VLT will soon give us more precise and reliable estimates of the age of the quasar environment. Emission lines from other elements, such as Fe and Mg can provide a better constraint to the age of the stars since their abundance depends more strongly on time. Fe is generated by supernovae type Ia on timescales of about 1 Gyr after the initial starburst (Greggio & Renzini 1983), whereas the production of Mg is dominated by supernovae types II, Ib and Ic. So the ratio of Fe to Mg should change dramatically after the first Supernovae Ia explode, i.e. 1 Gyr after the initial starburst.

We are presently carrying out a program to detect such lines in a sample of quasars at redshift between 5 and 6. By measuring the metal abundances we will then be able to set limits on the age of the stars and hence to the age of the Universe at redshifts as high as 6. From this age, constraints can then be put on H_0 , $\Omega_0 = \Lambda = 0$: for $H_0 = 65$, $\Omega_0 = 0.3$ and $\Lambda = 0.7$, the age of the Universe is ~ 1.2 Gyr at $z = 5$, while a model with $\Omega_0 = \Lambda = 0$ has an age exceeding 2 Gyr and a model of $\Omega = 1$ has an age of 0.7 Gyr.

4. Future developments and VLT contribution

The VLT will certainly give further contributions to our understanding of quasar formation and the reionization process. Future targets for VLT observations will be provided by the SDSS in the next few years. From the space density of luminous quasars at $z \sim 6$ we estimate that the SDSS will find a further ~ 10 luminous quasars in the redshift range $6 < z < 6.6$ over the 10,000 deg 2 of the total survey area (Fan et al. 2001). At even higher redshift ($z > 6.6$) the Ly α emission line moves out of the optical window and into the infrared. Thus the objects become very faint at optical wavelengths due to the absorption by neutral hydrogen gas in the foreground at lower redshifts. SDSS optical

photometry alone is not sufficient to find such objects but needs to be combined with near infrared colors. The next generation near-infrared sky survey, and in particular the UKIRT Infrared Deep Sky Survey (see the article by Stephen Warren in this issue of the Messenger) will provide the ideal complement to SDSS for the search of more distant sources. Indeed UKIDSS has amongst its aims the breaking of the redshift 7 barrier for quasars in order to determine the epoch of reionization.

Follow-up observations with 8-m-class telescopes giving high-resolution, high signal-to-noise ratio spectra of these luminous quasars in the Lyman series absorption regions will provide valuable probes of the reionization epoch (and beyond) and, in particular, measure the spatial inhomogeneity of the reionization process.

References

- Efstathiou, G. & Rees, M.-J. 1988, MNRAS, 230, 5P
- Fan, X. et al. 2001, AJ, 122, 2833
- Greggio, L. & Renzini A. 1983, A&A 118, 217
- Hamann, F. & Ferland, G. 1999, ARA&A, 37 487
- Hu, E.M. et al. 2002, ApJL, 568, 75
- Kennefick, J.D. et al. 1995, AJ, 110, 78
- Loeb, A. & Barkana, R. 2001, ARA&A, 39, 19L
- Pentericci, L. et al. 2002, AJ, 123, 2151
- York, D.-G. et al. 2000, AJ, 120, 1579
- Warren, S.J. et al. 1994, ApJ, 421, 412

Evidence for external enrichment processes in the globular cluster 47 Tuc?

DANIEL HARBECK, EVA K. GREBEL (Max-Planck-Institut für Astronomie, Heidelberg)
GRAEME H. SMITH (University of California/Lick Observatory, Santa Cruz, USA)

1. Abundance spreads in globular clusters

Globular clusters (GCs) have long had an appeal to astronomers as laboratories for studying stellar evolution. Part of their attraction arises not only from the vast number of stars that they contain, but also from the common properties that stars within a cluster are often thought to share. For example, in one standard text book (Carroll & Ostlie 1996) we find: "Every member of a given (star) cluster is formed from the same cloud, at the same time, and all with essentially identical compositions." Despite this paradigm, it has been known for 30 years that the element abundances among stars in a given GC can vary significantly. Globular clusters are the oldest star clusters known with ages on the order of the age of the universe. The chemical abundance pat-

tern among their stars is therefore an important clue to the first substantial production of heavy elements by massive stars in the early universe. Understanding the origin of the chemical inhomogeneity of GCs is therefore of interest for cosmology as well as stellar evolution.

The abundance of the elements carbon, nitrogen, and oxygen (C, N, and O) in particular show large variations among the red giants in many GCs (for a review see, e.g., Kraft 1994). These elements are of particular interest since they are the catalysts in the CNO cycle of nuclear fusion, in which hydrogen is converted into helium. The abundances of individual elements such as C and O can be measured directly by high-resolution spectroscopy, but this is very time-consuming even with large telescopes. An efficient alternative to probing the star-to-star scatter in the CNO

elements, especially for larger samples of stars, is to measure absorption band strengths of the CN molecule using low-resolution spectroscopy. The behaviour of this molecule can serve as a useful tracer of inhomogeneities in the individual CNO elements.

Absorption bands of CN occur at a number of places in the visible spectrum. As an example we show an integrated drift-scan spectrum of the moderate metallicity GC 47 Tuc in Figure 1, which was obtained in 2001 at the ESO 1.5m telescope with the B&C spectrograph. The CN absorption band at 3883 Å is clearly visible and is marked in the spectrum. Since the integrated light of 47 Tuc is emitted by a mix of stars, the existence of this strong 3883 Å feature indicates that stars with strong CN bands must be an important component of this cluster. The integrated spectrum, however, cannot tell us

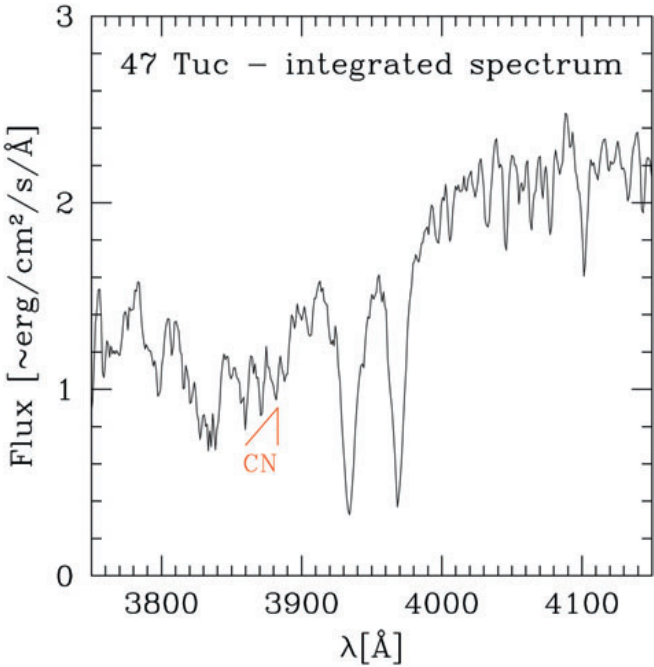


Figure 1: Integrated spectrum of 47 Tuc from the ESO 1.5m B&C spectrograph: The strong absorption band of the CN molecule below 3883 Å is clearly visible.

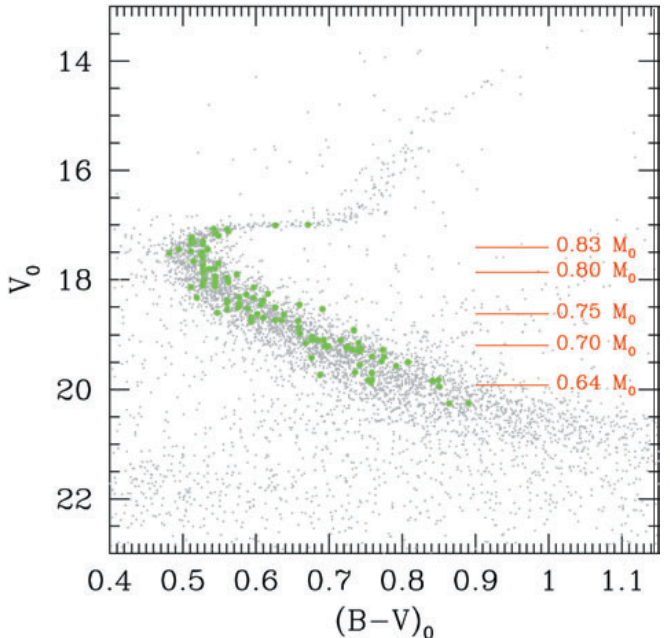


Figure 2: A color-magnitude diagram of 47 Tuc based on ESO/MPG 2.2m WFI observations. From the main sequence region we selected ~ 115 stars for follow-up spectroscopy at the VLT, which are marked by green dots. Approximate masses for stars at various locations on the main sequence are labelled in red using units of solar masses.

whether all 47 Tuc stars have enhanced CN absorption or whether the CN features vary from star to star. A star-by-star analysis is therefore mandatory.

Studies of CN absorption band strengths have been carried out for many stars in a variety of GCs. The first studies were conducted out with 2-meter-class telescopes and concentrated on bright red giant branch (RGB) stars. Pronounced star-to-star differences in CN content have been found for quite a few globular clusters (see Kraft 1994). In general, CN inhomogeneities in GCs are a common phenomenon and can be seen in moderately metal-poor clusters as well as in more metal-rich ones. With the use of increasingly larger telescopes scatter in the 3883 Å CN band strength has been found along the entire RGB of some clusters, even extending down to the subgiant branch (SGB) and the main sequence turn-off (MSTO) region (Cannon et al. 1998, Cohen 1999a, 1999b).

The origin of the CN abundance spread is still under investigation. A very good introduction to current discussions can be found in Cannon et al (1998), whose arguments we summarize here. Deep interior mixing is a promising candidate for producing surface CN enhancements in GC stars. In the hydrogen-burning region of a star the CNO-cycle alters the abundances of the elements C, N, and O. Although the CNO cycle is a catalytic process, it will increase the nitrogen content of a star, since the relatively slow $N \rightarrow O$ reaction produces a “bottleneck” that causes the build-up of nitrogen at the

expense of C and O. If interior mixing is sufficiently effective and extends deep enough within GC stars, then some CNO-processed material could be dredged up to the surface. The efficiency of deep mixing may vary from star to star; for instance stellar rotation, the rate of which may vary among cluster stars, could induce mixing. Current stellar models do not predict deep convective mixing for stars at the MSTO. Scatter in CN band strengths has nonetheless been detected for stars at the bright end of the main sequence in a few GCs such as 47 Tuc, M71, and NGC 6752. Thus, there are either other forms of mixing or diffusion processes occurring within main sequence GC stars, or else stellar interior processes are not the main instigator of the CN scatter.

Other explanations for the CN variations include primordial variations, self-enrichment and self-pollution. When referring to “primordial variations” we mean that the molecular cloud that formed a GC was not chemically homogeneous. For example, a GC might have formed from two colliding gas clouds having different chemical compositions, leading to a range of abundances in the subsequently formed stars. The time scale for star formation during the birth of a GC may have been long enough to allow for “self-enrichment” by exploding supernovae; stars that formed after such events could be enhanced in supernova ejecta. In these two scenarios the assumption that all stars in a cluster had the same initial chemical composition would not be valid. The problem of these scenarios is

the lack of abundance spreads in heavy elements such as iron in most clusters with CN variations. Finally, intermediate-mass stars undergo significant mass loss while on the asymptotic giant branch. Any CNO-processed material lost via a wind from such stars may be accreted by other stars in the GC and alter the chemical composition of their atmospheres without affecting their iron content.

Stars on the fainter part of the main sequence are the clue to the riddle of the CN variations. These stars experience hydrogen core burning only, which has two major contributing mechanisms: the pp-chain (which converts hydrogen into helium directly) and the CNO cycle. The CNO cycle requires much higher temperatures than the pp-chain to work efficiently. The contribution of the CNO cycle to the total energy production therefore is strongly reduced for lower mass stars due to their lower core temperatures. If CN variations among main sequence stars are caused by CNO-cycle nitrogen enrichment and deep mixing, one expects the scatter in CN to disappear along the MS simply because there is no mechanism left to alter the ratio of these elements. To investigate whether the CN variations do indeed disappear, we have measured CN absorption band strengths for stars in the globular cluster 47 Tuc as faint as 2.5 mag below the MSTO using the VLT.

2. Observations with the VLT

The FORS2 MXU multi-slit spectrograph at the Very Large Telescope

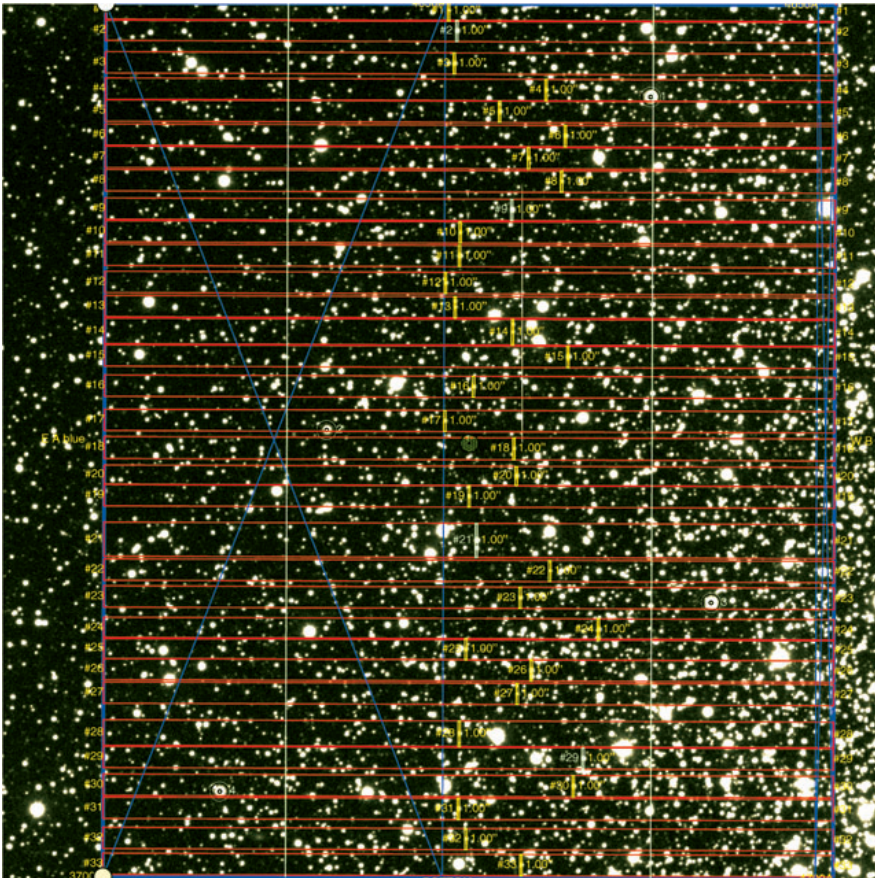


Figure 3: Example of one of the slit masks defined for our FORS/MXU observations. The mask was created using the FIMS software package.

(VLT) was used to obtain spectra for a sample of ~ 115 stars in the GC 47 Tuc. We chose this cluster for several reasons: (i) 47 Tuc stars are known to have inhomogeneities in CN absorption bands from the tip of the RGB down to a magnitude below the MSTO; the distribution of CN-rich and CN-weak stars is bimodal (e.g., Briley 1997 and references therein); (ii) 47 Tuc is relatively metal-rich by GC standards ($[Fe/H] = -0.7$ dex). Consequently the stars on the MSTO of 47 Tuc have atmospheres cool enough to form CN, in contrast to the hotter turn-off stars of the most metal-poor GCs.

To select candidate stars for spectroscopy we observed 47 Tuc in September 2000 with the ESO/MPG 2.2m telescope and the Wide Field Imager (WFI). The exposure time was 3×300 s in the filters Johnson B and V. The resulting color magnitude diagram (CMD) for chip #1 of the mosaic camera is shown in Figure 2. The subgiant branch, MSTO and the main sequence are clearly visible. The tip of the RGB is not represented since these stars were saturated on the CCD.

For the creation of the slit mask, three fields that overlap with our WFI observations were preimaged with FORS2 with a seeing better than 1 arcsec. The definition of slit masks for the FORS2/MXU is supported by a dedi-

cated software package (FIMS) which is distributed by ESO. Thanks to this software the mask creation process is very straightforward to do. Approximately 115 stars were selected for the VLT spectroscopy to be observed in three different slit masks. We show an example of a slit mask definition in Figure 3.

The VLT spectroscopy itself was carried out in service mode during several nights in September 2001. We chose the B600 grating of FORS, which provides a spectral resolution of 5 \AA . The wavelength range for all stars was chosen to cover at least $3700\text{--}5400 \text{ \AA}$. The alignment of the slit masks to the reference stars worked perfectly in service mode, even in the crowded environment of 47 Tuc. The final spectra of the stars have an exposure time of 3.5 hours.

3. CN abundance variations on the main sequence

Figure 4 shows example spectra of pairs of stars in three different luminosity ranges. In all ranges, stars with strong and weak CN absorption features at 3883 \AA can be found. A convenient tool to quantify the CN absorption strength is the $S(3839)$ index (Norris & Smith 1983) that compares

the flux $F(38)$ in the absorption feature with the flux $F(39)$ in a nearby comparison region just to the red of the CN band.

$$S(3839) = -2.5 \times \log_{10} \frac{F(38)}{F(39)}$$

According to Cohen (1999a,b), we used slightly different definitions of the passbands ($F(38)$ from $3861\text{--}3884 \text{ \AA}$ and $F(39)$ from $3884\text{--}3910 \text{ \AA}$) than Norris & Smith (1983) to avoid overlap of hydrogen absorption lines that are important for the hot MSTO stars. We formulated a zero-point-corrected CN index called $\delta S(3839)$, defined such that the stars with the weakest CN bands have an index value close to zero. Larger values of $\delta S(3839)$ indicate a stronger absorption in the CN band. In addition to the calculated index we visually assigned the CN absorption strength for each star to one of five classes ranging from CN-weak to CN-strong. It turned out that for a few stars the observations were too noisy for classification. For some stars, while we could identify the CN absorption, the classification was uncertain. The comparison between our visual classification and the measured absorption strength is shown in Figure 5. There is an excellent correlation between the two.

In Figure 6 we plot the $\delta S(3839)$ index versus the V-band magnitude of the stars along the main sequence of 47 Tuc. The differences in CN band strength that are already apparent in the example spectra in Figure 4 become well documented by the $\delta S(3839)$ index values, especially for the faintest stars. In particular, the bimodality of the distribution stands out: Main sequence stars in 47 Tuc seem to be either CN-strong or CN-weak. A bimodal CN distribution had been reported by other authors previously for stars on the RGB, the SGB, and of the MSTO of 47 Tuc. Our new VLT observations demonstrate that the existence of this CN bimodality is independent of the evolutionary state of the stars.

4. Conclusions

We have found a significant scatter in the CN absorption strength among main sequence 47 Tuc stars at all magnitudes in our survey. In relation to the stars near the main-sequence turn-off, the importance of the CNO cycle among the faintest stars in our sample is reduced by at least a factor of ten due to the decreased core temperature. Since this mechanism for altering the ratio between C and N diminishes substantially for the fainter stars, we conclude that stellar evolution is unlikely to be the only process at work that causes the star-to-star variations in CN band strength. One concern of this in-

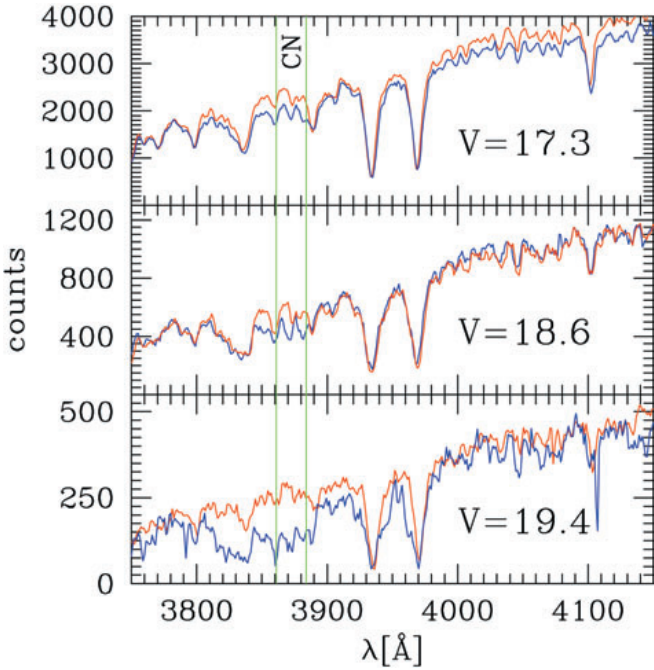


Figure 4: Spectra of main sequence stars in 47 Tuc: we show examples of CNrich stars (blue) and CN-poor stars (red) at three different magnitudes on the main sequence. Note the clear differences in the $\lambda 3883\text{\AA}$ CN band, in particular for the faintest stars.

terpretation is that a decrease in the CN abundance spread among the fainter stars along the main sequence may be hidden by increased CN association in the lower-temperature atmospheres of these stars. Model atmosphere analyses of the observed stars could address this question. It would also be valuable to observe the CN band strengths of stars one magnitude fainter than the current sample. For example, our simple calculations predict a decrease of the CNO-cycle efficiency for such stars by a factor of 100 compared to the MSTO. If such deep observations also find CN variations, then they would verify our results.

While internal stellar evolution seems unlikely as the origin of the CN variations in 47 Tuc, external processes may have played an important role. Unfortunately, from the low resolution spectroscopy alone, the true origin of the enhanced abundances of the CN-strong stars cannot be determined. The next step is to search for the fingerprint of different enrichment processes: cluster self-enrichment by massive stars versus accretion of material ejected in winds from intermediate-mass stars. High resolution spectroscopy with UVES at the VLT might provide answers to these questions.

Carroll, B. W. & Ostlie, D. A. 1996, An Introduction to Modern Astrophysics, Addison-Wesley.

Cohen, J. G. 1999a, AJ, 117, 2428

Cohen, J. G. 1999b, AJ, 117, 2434

Kraft, R. P. 1994, PASP, 106, 553

Smith, G. H. & Norris, J. 1983, ApJ, 264, 215

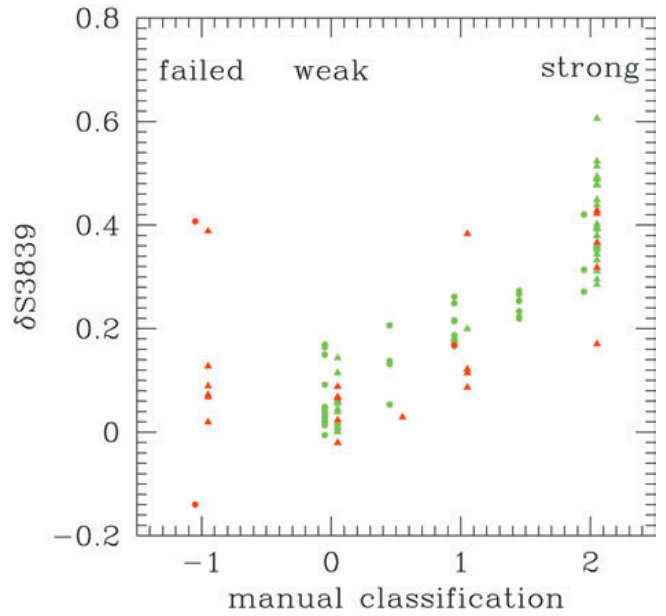


Figure 5: Visual classification vs. calculated CN band strength: Green dots represent secure measurements of the CN absorption lines; red dots indicate that the measurement may be dominated by systematic effects (e.g., strong hydrogen lines). Stars with ≥ 18.5 mag are plotted with triangles, brighter stars are plotted with circles. Note the excellent correlation between the measured absorption band strength and the visual classification.

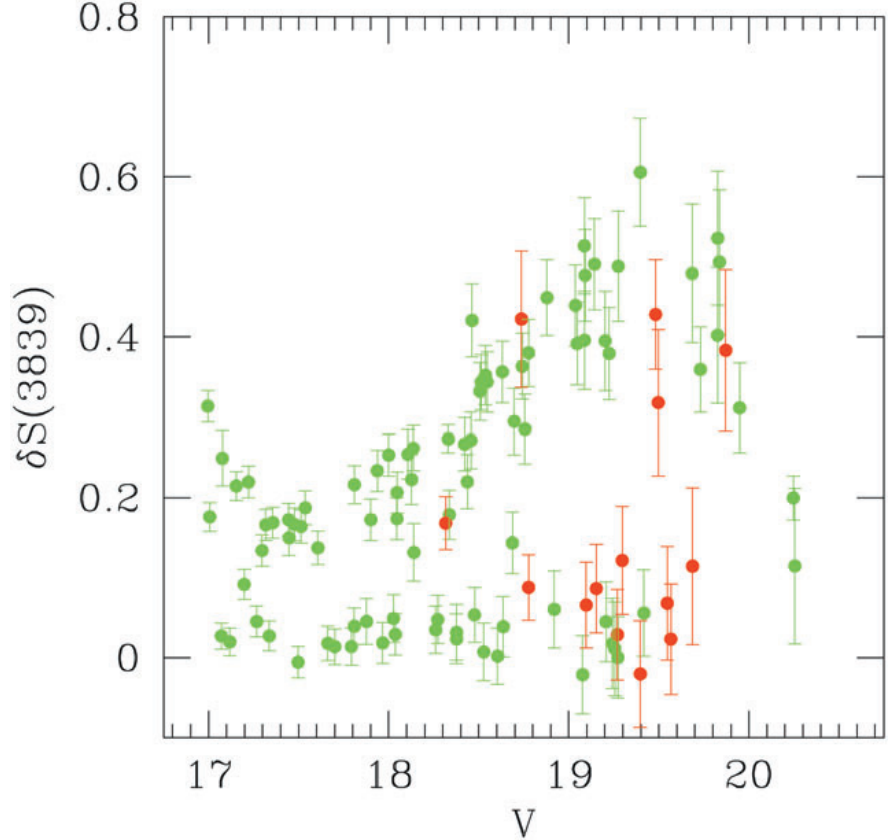


Figure 6: The $\delta S(3839)$ CN index is shown plotted against V magnitude for stars on the main sequence of 47 Tuc. Secure measurements are plotted with green dots; red dots represent uncertain measurements. Note the bimodal distribution of the CN absorption strengths, with stars falling into two relatively distinct groups on the basis of the CN index.

References

- Briley, M. M. 1997, AJ, 114, 1051
 Cannon, R. D., Croke, B. F. W., Bell, R. A., Hesser, J. E., & Stathakis, R. A. 1998, MNRAS, 298, 601



Aerial view of Paranal, with the Llullaillaco volcano (6730 m) in the background, 190 km distant. (Photo: G. Hudepohl.)